A Tri-Port Wearable Tag for Indoor Communication with Power Delivery Through Near-Field and Far-Field Energy Harvesting

A Tri-Port Wearable Tag for Indoor Communication with Power Delivery through Near-Field and Far-Field Energy Harvesting

Giacomo Paolini
DEI "Guglielmo Marconi"
University of Bologna
Cesena, Italy
giacomo.paolini4@unibo.it

Francesca Benassi
DEI "Guglielmo Marconi"
University of Bologna
Bologna, Italy
francesca.benassi9@unibo.it

Giulia Battistini
DEI "Guglielmo Marconi"
University of Bologna
Bologna, Italy
giulia.battistini13@unibo.it

Elisa Augello
DEI "Guglielmo Marconi"
University of Bologna
Bologna, Italy
elisa.augello2@unibo.it

Diego Masotti
DEI "Guglielmo Marconi"
University of Bologna
Bologna, Italy
diego.masotti@unibo.it

Alessandra Costanzo
DEI "Guglielmo Marconi"
University of Bologna
Bologna, Italy
alessandra.costanzo@unibo.it

***Abstract*—This work introduces an innovative hybrid simultaneous wireless information and power transfer architecture that integrates both near-field and far-field wireless power transfer mechanisms into a single compact receiving tag. The system features a dual-mode energy harvesting design: a resonant coil operating at 13.56 MHz for efficient near-field power transfer, and a cross-polarized antenna system for far-field energy harvesting and data communication in the 2.4 GHz band. The antenna employs a dual-fed configuration that combines coaxial and microstrip feeding techniques, optimizing radiation performance and polarization diversity for robust communication. Detailed electromagnetic simulations are corroborated by antenna and power transfer measurements, which demonstrate the effectiveness of the design. This multifunctional tag is tailored for low-power applications such as Internet of Things devices, radiofrequency identification systems, and wireless sensor networks, offering a highly integrated solution for simultaneous energy acquisition and wireless data transmission.**

Keywords—automotive, industrial, ISM, localization, RFID, SWIPT, tag, wearable, WPT.

I. Introduction

The convergence of wireless energy transfer and communication technologies has recently catalyzed the evolution of simultaneous wireless information and power transfer (SWIPT) systems, emerging as a pivotal paradigm for future applications in domains such as the Internet of Things (IoT), Industry 4.0, automotive applications, and intelligent healthcare. The increasing demand for self-sustaining, battery-less devices capable of operating under dynamically changing environmental and spatial conditions has stimulated considerable research into highly integrated, energy-efficient architectures that can support both uninterrupted energy supply and dependable data communication.

Advancements in low-power electronics and integrated circuit technologies have rendered it feasible to sustain wireless nodes via ambient or dedicated radiofrequency (RF) energy sources. Among wireless power transfer (WPT) techniques, near-field (NF) solutions [1], based on inductive or capacitive coupling, offer high efficiency over short distances, whereas far-field (FF) approaches [2] leverage propagating electromagnetic waves to achieve power transfer over extended ranges, with enhanced spatial coverage. Nonetheless, most current SWIPT implementations employ a single power transfer modality, thus limiting their adaptability and robustness in realistic, heterogeneous environments [3].

To address these limitations, this work proposes a novel dual-mode SWIPT system that integrates both NF and FF WPT modalities within a unified, compact and wearable radiofrequency identification (RFID)-based platform. The proposed architecture incorporates a 13.56 MHz (high frequency – HF band) resonant inductive coil for efficient NF power harvesting and a 2.4 GHz (ultra-high frequency – UHF band) cross-polarized antenna for FF RF energy acquisition and bidirectional data communication. The antenna design employs a hybrid coaxial–microstrip feeding structure, enabling polarization diversity; this hybrid energy harvesting framework allows for dynamic adaptation to variable RF sources and operating conditions, thereby ensuring continuous device operability across a broad spectrum of application scenarios, including smart manufacturing environments, indoor asset tracking, automotive sensing, and context-aware monitoring systems. Specifically, in the domain of healthcare, the wearable SWIPT-enabled tag is engineered to support real-time 3D localization, fall detection, and behavioral analysis of tracked users. Experimental evaluations conducted in realistic indoor conditions validate the efficacy of the proposed system, demonstrating valuable energy harvesting efficiency.

Finally, this work contributes a significant step toward the realization of fully integrated, dual-mode SWIPT platforms for next-generation wearable, RFID, and ubiquitous sensing applications.

II. Dual-Port Antenna Design and Measurements

A. Dual-Port UHF Antenna Project

The proposed dual-port SWIPT patch antenna features a dual-polarized radiating structure operating in the 2.4 GHz industrial, scientific and medical (ISM) band, designed to support both wireless power reception and data communication. The antenna is fabricated on a Rogers RO3003 substrate ($\varepsilon_r = 3$, $tan(\delta) = 0.001$, thickness: 0.76 mm); the flexibility of this substrate, due to its limited thickness, makes this tag suitable for wearable applications allowing a more comfortable use and functionality.

The overall size of the receiving (RX) tag, including the near-field coil that will be described in the following section, is 6.2 × 6.2 cm² [4].

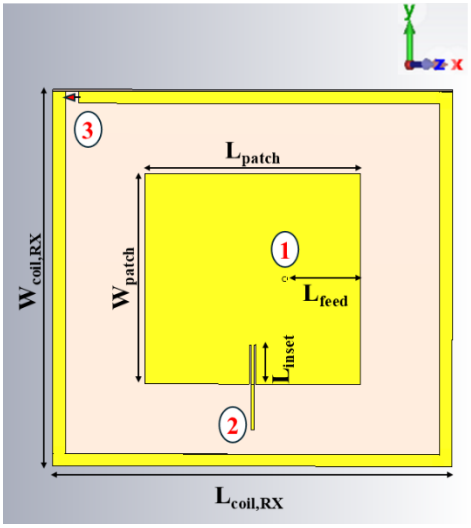

Fig. 1. Configuration of the tri-port system, featuring a dual-fed antenna operating at 2.4 GHz —dedicated to data communication on port 1 and far-field energy harvesting on port 2— and a receiving coil tuned to 13.56 MHz for near-field wireless power transfer via port 3.

The layout of the flexible tag reported in Fig. 1 shows all the three ports of the dual-band tag:

- Antenna Port 1 is dedicated to communication and is realized through a coaxial feed (50-Ω impedance for interfacing with commercial transceivers, i.e., the Texas Instruments CC2530); it works with a linearly polarized field along the *x*-axis.
- Antenna Port 2 is intended for far-field energy harvesting and uses microstrip feed. It will be connected to a RF-to-DC rectifier composed of lumped and distributed components and generates a linearly polarized field along the *y*-axis.
- Port 3 is the input of the NF receiving coil, which will be described in the next section.

The key design parameters shown in Fig. 1 include: L_{patch} = 33.5 mm, W_{patch} = 34.8 mm, L_{inset} = 6.5 mm, and L_{feed} = 5 mm. The microstrip line at port 2 has a width of 0.5 mm, yielding a characteristic impedance of approximately 109 Ω. This value, together with the slight difference between the L_{patch} and W_{patch} values, is selected to guarantee adequate electrical isolation between the two feeding ports, while also facilitating proper impedance matching at both input interfaces; conversely, a standard 50 Ω impedance for the transceiver connection has been adopted.

In order to optimize the NF WPT efficiency, the antenna's ground plane was reduced to 50 × 50 mm² behind the planar antenna. Further reduction in size was avoided in order to maintain the required antenna gain for both polarization states. A careful design trade-off was found to guarantee a balance between the FF radiation characteristics and the inductive NF coupling efficiency.

B. Antenna and FF UHF Harvesting Measurements

The measured scattering parameters (measured on 50-Ω-loads) of the two-port antenna are reported in Fig. 2. The minimum of the reflection coefficient absolute value ($|S_{11}|$) for the coaxial-fed antenna exploited for communication is located at 2.40 GHz ($|S_{11}|$ = –10 dB), whereas for the energy harvesting (EH) antenna it occurs at 2.49 GHz ($|S_{22}|$ = –15.6 dB).

This frequency spacing helps guarantee sufficient port decoupling: the absolute value of the transmission coefficient ($|S_{21}|$) between the two ports is lower than –12 dB over the entire 2.4 GHz band, as can be seen in Fig. 2; in particular, $|S_{21}|$ is equal to –15.3 dB and –12.6 dB at 2.40 GHz and 2.49 GHz respectively.

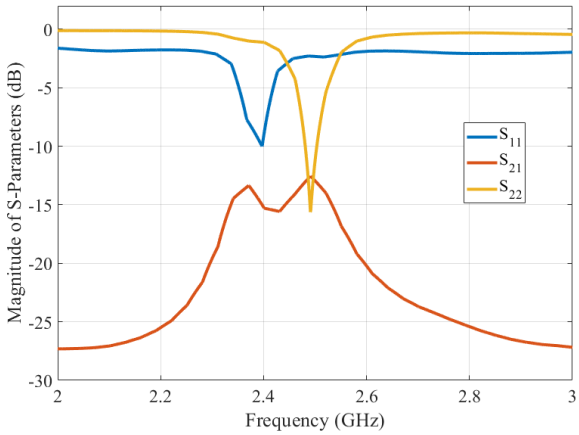

Fig. 2. Measured magnitude of the scattering parameters for the dual-port 2.4 GHz antenna (Ports 1 and 2 of the RX tag), normalized to 50 Ohm.

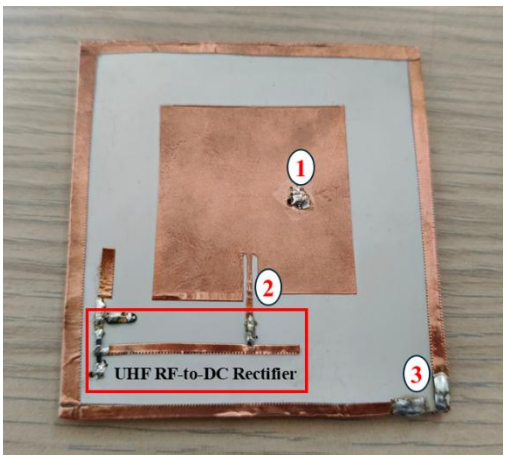

Fig. 3. Photograph of the front layer of the SWIPT tag realized with adhesive copper, with the dual port antenna (Ports 1 and 2) and the RX coil (Port 3), with the UHF RF-to-DC rectifier highlighted. The lumped and distributed components of HF rectifier have been placed on the bottom layer of the tag.

Regarding the FF EH part, the RF-to-DC rectifier working at 2.45 GHz has been designed on the same Rogers RO3003 substrate of the antenna (highlighted in Fig. 3); in particular, it is composed of a matching network (C_{MN} = 0.26 pF, an 11-mm-long parallel open stub, a 22.3-mm-long series transmission line), a shunt diode D_1 (Skyworks Schottky diode SMS7630-079LF), and a low-pass filter with L_1 = 31 µH, and C_{L1} = 1 nF. All the distributed elements of the circuit have a width of the microstrip lines equal to 1.4 mm.

The UHF harvesting measured results revealed a noticeable RF-to-DC power conversion efficiency (PCE) $\eta_{RF\text{-}to\text{-}DC,2.45GHz}$ of the UHF rectifier, calculated as:

$$\eta_{RF-to-DC,2.45GHz} = \left(\frac{P_{out2,DC}}{P_{IN,2.45GHz}}\right) \cdot 100 \qquad (1)$$

where $P_{out2,DC}$ represents the DC output power calculated over the optimum output load (849 Ω), and $P_{IN,2.45GHz}$ the UHF power at the input of the RF-to-DC rectifier.

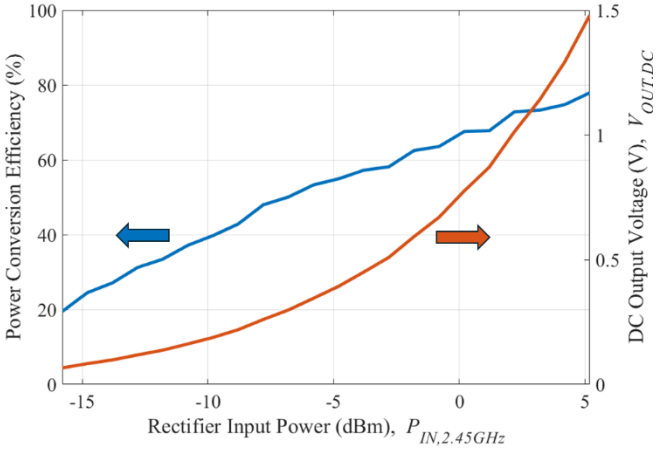

Fig. 4. Measured PCE ($\eta_{RF\text{-}to\text{-}DC,2.45GHz}$) and output voltage ($V_{OUT,DC}$) for the 2.45 GHz UHF harvester.

These results, as illustrated in Fig. 4, allow to harvest about 40 µW and 5 µW of DC power for an RF input at the rectifier equal to –10 dBm and –16 dBm, respectively, confirming the feasibility and robustness of the proposed design.

III. Validation of the NF HF WPT System

Two different transmitting (TX) coils were employed in the experimental setups to evaluate NF WPT performance:

- For TX-1: a smaller curved 1-turn coil measuring 5.2 × 10.0 cm^2, realized with a 0.70-mm-diameter Litz wire, as the one employed in [5];
- For TX-2: a larger planar 1-turn coil realized on an Isola DE104 substrate (ε_r = 4.46 and $tan(\delta)$ = 0.020, thickness: 1 mm) with dimensions of 20 × 13 cm^2 (coil width: 3 mm).

Consequently, TX-1 is a Litz-wire coil resonant with a parallel capacitor of 430 pF, all in series with an inductor of 140 nH, whereas TX-2 is composed of a coil driven in parallel-resonant condition using a capacitance equal to 22 pF.

The RX equivalent circuit on the tag side consists of a resonating system composed of a 1-turn RX square coil of dimensions L_{coil} = W_{coil} = 6.2 cm, width of 2 mm, and copper thickness of 35 µm (coil equivalent inductance L_{RX} = 127.2 nH and resistance R_{RX} = 0.05 Ω at 13.56 MHz) and a parallel capacitor C_{RX} = 1.12 nF, loaded by the HF rectifier, which is made up of a series diode D_2 (Skyworks Schottky diode SMS3922-079LF), followed by a low-pass section with L_2 = 2.2 µH, and C_{L2} = 10 nF.

Coupling measurements between the TX and RX coils were conducted under different conditions. Adopting TX-1 at the transmitter side, the RX coil was positioned at a single fixed location with a separation distance of 3 cm from TX center. For this setup (Fig. 5), an overall RF,TX-to-DC efficiency $\eta_{RF,TX\text{-}to\text{-}DC,13.56MHz}$ of 30.9% has been achieved, which has been calculated as:

$$\eta_{RF,TX-to-DC,13.56MHz} = \left(\frac{P_{out3,DC}}{P_{TX,13.56MHZ}}\right) \cdot 100 \qquad (2)$$

where $P_{out3,DC}$ represents the DC output power calculated over the optimum output load (637 Ω), and $P_{TX,13.56MHz}$ the power transmitted (here, 20 dBm) by the RF generator (Keysight N5183B).

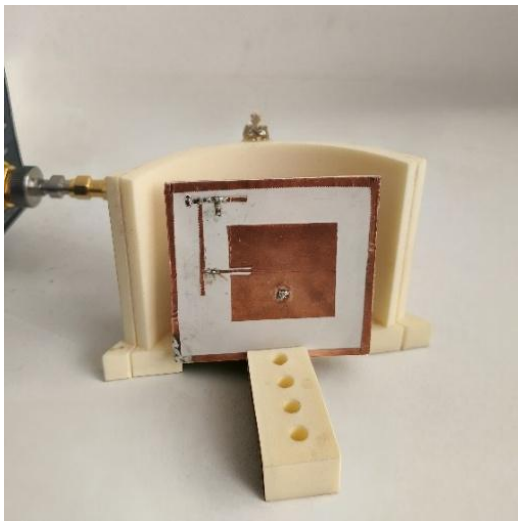

Fig. 5. NF-powering measurement setup adopting TX-1 prototype (Litz wire incapsulated into a polymeric 3D-printed support) as transmitter coil in the HF band.

In the case of larger planar TX coil (TX-2), the RX coil was placed in direct contact with the Isola DE104 substrate, and the transmission efficiency was characterized for multiple positions (visible in Fig. 6) to evaluate spatial variation in the magnetic coupling. The resulting $\eta_{RF,TX\text{-}to\text{-}DC}$ values are reported in Tab. 1 for the five different positions. The RF power transmitted by the RF analog signal generator at 13.56 MHz is equal to 20 dBm, as in the previous case. These efficiencies are calculated over an output load equal to 490 Ω, which is the optimized value for Position 1 (the geometric center of TX-2).

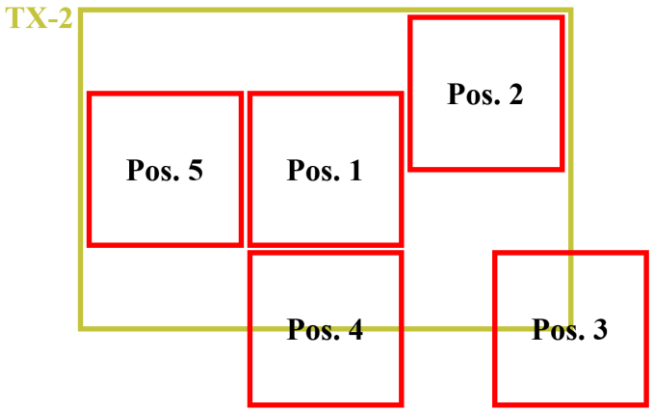

Fig. 6. Different testing positions for coupling and PCE measurements between TX-2 (yellow) and RX (red).

It is possible to notice from Tab. 1 that the overall efficiencies reached with TX-2 are lower with respect to the ones achieved with TX-1; this is mainly due to the fact that the TX-2 coil has significantly larger dimensions compared to the RX one.

TABLE I. PERCENTAGE PCE FOR TX-2 FOR DIFFERENT RX POSITIONS

Position	***1***	***2***	***3***	***4***	***5***
$\eta_{RF,TX\text{-}to\text{-}DC,13.56MHz}$ ***(%)***	2.17	21.42	0.002	0.08	11.76

In fact, it has been observed that magnetic coupling is significantly enhanced when the receiving coil is placed near the edges of the transmitting one, particularly near the shorter sides (Pos. 5) or corners (Pos. 2), rather than at its center (Pos. 1). This behavior arises because the magnetic flux lines tend to spread outward at the edges, increasing the effective flux linkage with the receiver. In contrast, positioning the receiving coil at the center where the field is more uniform and perpendicular, results in less total flux being captured, particularly when the receiver is significantly smaller than the transmitter. As a result, the fringe regions of the transmitting coil often provide a more favorable configuration for maximizing mutual inductance and power transfer.

CONCLUSION

This work introduces a hybrid SWIPT architecture that effectively integrates both NF and FF energy harvesting mechanisms into a single, compact receiving tag, realized with a flexible material. The system features a dual-mode energy harvesting design that includes a 13.56 MHz resonant coil for NF power transfer and a cross-polarized antenna for FF energy harvesting and data communication at 2.4 GHz.

The use of a dual-fed antenna configuration, incorporating both coaxial and microstrip feeding techniques, optimizes performance across both polarization states, ensuring robust communication. The design's efficacy is demonstrated through electromagnetic simulations and experimental validation. Specifically, NF-WPT with similarly sized RX and TX coils achieves a 31% conversion efficiency (calculated based on a source power equal to 100 mW), while FF-WPT provides a 40% conversion efficiency (with regards to an input power at the rectifier of 100 μW).

This highly integrated tag is tailored for low-power applications such as IoT devices, RFID systems, and wireless sensor networks, offering an efficient and compact solution for simultaneous energy harvesting and wireless data transmission. The results underscore the potential of this dual-mode architecture to improve the efficiency and versatility of wireless harvesting systems in real-world applications, paving the way for next-generation wireless communication and energy harvesting technologies.

ACKNOWLEDGMENT

This work was partly funded by the European Union (EU) under the NextGenerationEU programme, the Italian Ministry of Enterprises and Made in Italy (MIMIT), and the University of Bologna within the framework of the "AlmaValue for RR" project "WirelessLOC" (CUP: C38H23000710002), and partly by the EU (NextGenerationEU) under the Italian National Recovery and Resilience Plan (NRRP), Mission 4, Component 2, Investment 1.3 (CUP: J33C22002880001), partnership on "Telecommunications of the Future" (PE00000001 – program "RESTART").

This study was carried out also within the Spokes 7 and 13 of the MOST (Sustainable Mobility National Research Center) and received funding from the European Union under the NextGenerationEU programme (National Recovery and Resilience Plan (NRRP) – Mission 4 Component 2, Investment 1.4 – D.D. 1033 17/06/2022, CN00000023).

REFERENCES

[1] N. Shinohara, "Trends in Wireless Power Transfer: WPT Technology for Energy Harvesting, Millimeter-Wave/THz Rectennas, MIMO-WPT, and Advances in Near-Field WPT Applications," IEEE Microwave Magazine, vol. 22, no. 1, pp. 46-59, January 2021.

[2] X. Gu, S. Hemour, and K. Wu, "Far-Field Wireless Power Harvesting: Nonlinear Modeling, Rectenna Design, and Emerging Applications," Proceedings of the IEEE, vol. 110, no. 1, pp. 56-73, January 2022.

[3] M. Wagih, G. S. Hilton, A. S. Weddell, and S. Beeby, "Dual-Band Dual-Mode Textile Antenna/Rectenna for Simultaneous Wireless Information and Power Transfer (SWIPT)," IEEE Transactions on Antennas and Propagation, vol. 69, no. 10, pp. 6322-6332, October 2021.

[4] G. Paolini, G. Battistini, D. Masotti, S. Scanzio, G. Cena, and A. Costanzo, "Design of a Dual-Band Tri-Port Tag for Near-Field Energy Harvesting and Far-Field SWIPT," 2025 URSI AP-RASC, Sydney, Australia, 2025.

[5] A. Pacini, F. Benassi, D. Masotti, and A. Costanzo, "Design of a RF-to-dc Link for in-body IR-WPT with a Capsule-shaped Rotation-insensitive Receiver," 2018 IEEE/MTT-S International Microwave Symposium - IMS, Philadelphia, PA, USA, 2018.